Steel processed by water jet cavitation with ultrasonic irradiation

[1]Masataka Ijiri*; [1]Daisuke Nakagawa; [1]Kumiko Tanaka; [1]Toshihiko Yoshimura;

[1]Tokyo University of Science, Yamaguchi, JAPAN;

Abstract

Alloy steels for machine structural is used for industrial equipment. However, the operating environment is often harsh, requiring the development and application of various surface treatments. The authors focus on the use of water jet cavitation (WJC) with ultrasonication. WJC technology enables the generation of high pressure during cavitation collapse near the surface when a water jet ejected from a nozzle impacts a metal surface. This pressure causes a slight deformation in the impacted surface region and introduces a compressive residual stress due to the elastic constraints of the underlying and surrounding metal. If ultrasonic irradiation is applied to WJC bubbles with diameters of several hundred microns, the bubbles are subjected to alternating high and low sound pressures, which leads to a high-pressure and high-temperature reaction field. This technique is referred to as multifunction cavitation (MFC). The authors have reported several characteristics of specimens processed by MFC to date. For example, titanium oxide powder, which is widely used as a photocatalyst, can be fabricated in the form of nanoparticles by MFC. In addition, the indium tin oxide (ITO) film deposited on the transparent electrode mounted on liquid crystal displays can be melted by MFC treatment, leading to the release of indium, which has a low melting point. In present study, the compressive residual stress and corrosion resistance of Cr-Mo and Ni-Cr-Mo steels were improved by MFC treatment. Moreover, the authors compared conventional WJC technology to MFC technology. MFC was found to lead to higher compression residual stresses and higher corrosion resistances compared to conventional WJC. The corrosion resistance was revealed by the formation of an oxide film through selective oxidation and the concomitant reduction of surface defects. The oxide coating formed by a reaction between the dissolved oxygen in water with Cr on the metal surface during processing.

Keywords: Water jet cavitation; Multifunction cavitation; Low-alloy steel; Surface reforming

Introduction

Alloy steel for machine structural has been used for a wide range of machine parts mainly automobile parts. The improvement of fatigue characteristics isn't always satisfactory with the conventional surface modification at present, because of the use environment of this material is harsh year by year. To solve this problem, development of surface treatment and its practical application are expected. As one method, the authors take particular note of a multifunction cavitation (MFC) method with high-temperature and high-pressure microjet (MJ) which features both water jet cavitation (WJC) and ultrasonic cavitation (UC) [1]. In the WJC technology, high pressure occurs when the cavitation caused by high pressure water jetted from a nozzle collapses on the metal surface. This impact pressure results in slight plastic deformation of the surface layer and generates compressive residual stress by an elastic restraining force from the lower layer portion and the surroundings. When the compression force is converted to compression deformation, the deformation returns to its original state after the cavitation collapse; however, if a small amount of plastic deformation occurs, then compressive residual stress is generated after cavitation collapse. When WJC is applied to a welded part where tensile residual stress exists or a surface finished by surface grinding, the tensile residual stress on the surface is reduced and a compressive residual stress is produced. As a result, fatigue strength [2] and stress corrosion cracking resistance [3] are improved. Other than WJC technology, there are vibration cavitation called UC and laser induced cavitation. In the vibration cavitation, there are low sound pressure and high sound pressure in the liquid, because ultrasonic vibration generates strong and dense longitudinal waves in the liquid by applying strong ultrasonic waves in the liquid. Bubbles under low sonic pressure are expanded and then quickly shrink under high pressure. After repeating isothermal expansion or adiabatic compression, the bubbles collapse. UC is typically applied in chemistry, biotechnology, and medicine, using several microsize bubbles with a high temperature reaction field [4] generated by repetition of the expansion or contraction processes. Recently, we have developed a cavitation method with high-temperature and high-pressure microjets (MJs) that features both WJC and UC. This cavitation technique is so-called the mechanical and electrochemical cavitation method because it has both of mechanical action by MJ with high pressure of WJC and electrochemical action [5] by MJ with high temperature reaction field of UC. Moreover, it can be called MFC because it has new functions given to various materials. The

*Corresponding Author, Masataka Ijiri: ijiri@rs.tusy.ac.jp

authors have reported several characteristics of specimens processed with MFC so far. For example, firstly, titanium oxide powder is widely used as a photocatalytic material. It has been reported that the titanium oxide powder can be microfabricated to nano level when processed with MFC [6]. Secondly, the ITO film is a material applied to the transparent electrode mounted on the liquid crystal panel. It has also been reported that melting and releasing of indium having a low melting point occurs when an ITO (Tin-doped Indium Oxide) film coated on a transparent electrode mounted on a liquid crystal panel is subjected to MFC treatment [1]. In present study, the compressive residual stress and corrosion resistance of Cr-Mo and Ni-Cr-Mo steels were improved by MFC treatment. Moreover, the authors compared conventional WJC technology to MFC technology.

Experimental methods

The material used for these tests was Cr-Mo steel (SCM435) and Ni-Cr-Mo steel (SNCM630), both structural steels, the chemical compositions of which are shown in Table 1.

Table 1. Chemical composition of the low-alloy steels used in this work (mass%).

	C	Si	Mn	P	S	Ni	Cr	Mo	Cu	Fe
SCM435	0.37	0.32	0.81	0.014	0.012	0.012	0.95	0.15	0.14	Bal.
SNCM630	0.29	0.24	0.44	0.11	0.018	2.93	3.01	0.56	0.03	Bal.

Figure 1 is a schematic diagram of the equipment used for MFC processing. This equipment was similar to a conventional WJC apparatus, in that a jet of room temperature tap water was discharged from a nozzle at 35 MPa. The nozzle diameter was 0.8 mm. The distance between the nozzle and the specimen was 65 mm. The size of the water tank was 60×45×37 mm^3, and it was filled with tap water. In MFC treatment, an ultrasonic transducer is placed next to the water jet nozzle for conventional WJC, and ultrasonic waves are propagated to the water jet flowing from the nozzle. The ultrasonic wave had an output of 225 W and frequency of 28 kHz. As shown in Figure 2, bubbles from WJC isothermally expand when the sonic pressure due to ultrasonic irradiation exceeds the Blake threshold, and after the bubbles expand to a certain size, Rayleigh shrinkage occurs rapidly (adiabatic compression). The flow cavitation, including the hot spot, becomes MFC by the repetition of isothermal expansion and adiabatic compression. At the same time that the MFC begins to collapse, it approaches the specimen surface. Figure 3 shows the bubble shape change from photographs taken by a high-speed camera during bubble collapse into an aspheric shape [7]. As the volume of the bubble decreases, a MJ with a columnar shape is formed and impinges on the specimen surface. This phenomenon is referred to as micro-forging because the MJ provides high-temperature and high-pressure processing in a microscopic area. Conventional WJC produces large high-pressure bubbles (diameter of several hundred micrometers at approximately 1,000 MPa), whereas bubbles produced with conventional UC are small (several micrometers) with high temperature (several thousand degrees Celsius). In contrast, the MJ that occurs in a bubble during MFC is a deforming liquid-phase body similar to a liquid jet (column) at the terminal stage of bubble collapse, and the interior temperature and pressure of the bubble become high (several thousand degrees Celsius and approximately 1,000 MPa, respectively). The processing time for all three methods was 2 min. Residual stress was measured by the full-width at the half-value breadth method from the (211) lattice spacing strain using Cr Kα X-ray diffraction (MSF-3M, Rigaku Corporation). Micro Vickers hardness tests were performed at room temperature under a load of 1.96 N for 10 s. The hardness values were averaged from eight measurements after the minimum and maximum of ten measurements were discarded. In addition, hardness measurements near the surface after processing were performed after slight mechanical polishing to remove the oxide film and peening marks formed during processing. Microstructure observations were conducted using optical microscopy (OM) and scanning electron microscopy (SEM; S-4800, Hitachi, Ltd.). Before observation, the specimens were etched in 5 vol% Nital. The specimens used for all analyses after processing were cut to 1×1 cm^2. For dissolved oxygen (DO) measurement, a portable type DO analyzer (OM–71, Horiba, Ltd.) was used. This measurement was carried out by appropriately collecting treated water in which cavitation occurred within a reactor made of SUS304 for a processing time of 30 min.

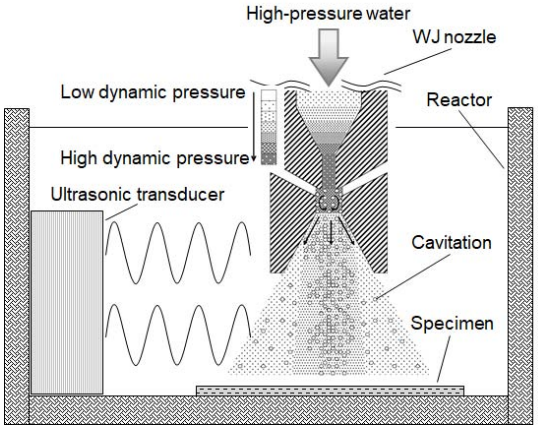

Figure 1. Equipment employed for surface machining by water jet cavitation under ultrasonication.

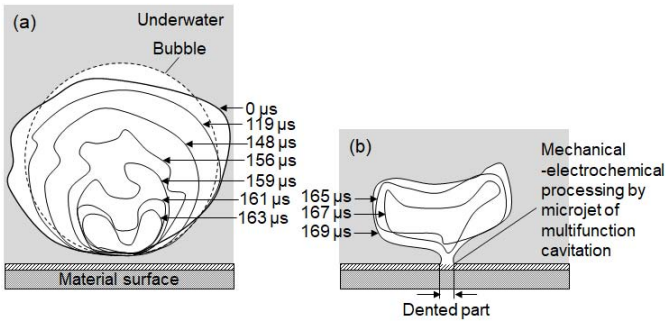

Figure 3. Images showing the aspherical collapse of a bubble at time intervals of (a) 0-163 μs and (b) 165-169 μs.

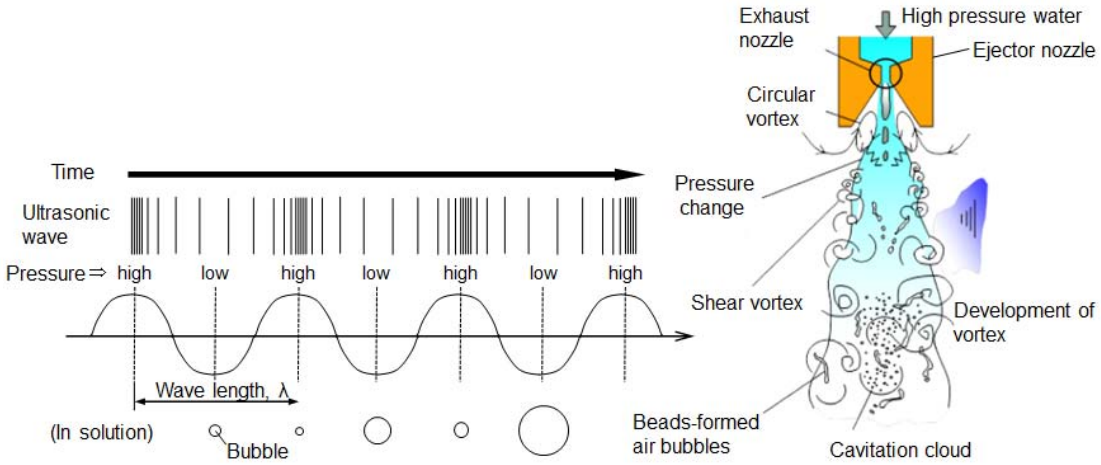

Figure 2. Multifunction cavitation mechanism.

Results and discussion

Table 2 shows the results of residual stress measurements. To further increase the compressive residual stress generated after WJC and MFC processing, the specimen surface was first subjected to hard grinding, which imparted tensile residual stress by a shakedown effect. These measurements were conducted in a state without rust on the specimen surface just after each processing and were performed in a direction parallel to the grinding direction. It was confirmed that grinding imparted a tensile residual stress in the grinding direction of the unprocessed specimens, while a compressive residual stress was imparted in the vertical direction. In WJC and MFC processing, compressive residual stress is generated when the specimen surface is compressed by the pressure from cavitation because the MJ applies force in the lateral direction, leading to plastic deformation around the region that is elastically constrained by its surroundings. Figure 4 shows the change in the micro Vickers hardness for each processed surface in the depth direction, but does not include the oxide film and peening marks. In the hardness of the near-surface region in the unprocessed specimen, SCM435 was 246 HV, and SNCM630 was 256 HV. The hardness distribution of the unprocessed specimen remained unchanged in the depth direction. It is considered that the unprocessed specimen is not significantly influenced by the strong surface grinding that was performed to impart tensile residual stress. The hardness in the near-surface region of the WJC-processed SCM435 was 271 HV. The hardness decreased at a depth of ca. 0.75 mm from the surface layer. On the other hand, the hardness in the near-surface region of the MFC-processed specimen was 276 HV. The hardness decreased at a depth of ca. 0.5 mm from the surface layer. This hardness change depends on the value (compressive stress field) where compressive residual stress was added in the depth direction. The compressive stress field was deeper in WJC than MFC. The compressive stress field occurred at a depth of ca. 0.5 mm after WJC processing, and it occurred at a depth of ca. 0.25 mm after MFC processing. About the depth of ca.

0.50 mm of WJC processed specimen, it is considered that the hardness decreased compared with the abrasive material due to voids and cracks. The reason why the hardness decreased from the depth of ca. 0.5 mm in the specimen after WJC processing is considered to be the influence of voids and cracks inside the specimen. Recently, the authors report that voids and cracks tend to form inside the specimen after WJC processing [8]. The hardness in the near-surface region of the WJC-processed SNCM630 was 270 HV. The hardness decreased at a depth of ca. 1.00 mm from the surface layer. On the other hand, the hardness in the near-surface region of the MFC-processed specimen was 264 HV. The hardness decreased at a depth of ca. 1.00 mm from the surface layer. The compressive stress field occurred at a depth of ca. 0.75 mm after WJC processing, and it occurred at a depth of ca. 0.50 mm after MFC processing.

Table 2. Compressive residual stress of specimens before and after various treatments (MPa).

		SCM435	SNCM630
As received after grinding	Vertical direction	-173	-238
	Parallel direction	+202	+155
UC		-216	-196
WJC		-361	-450
MFC		-293	-481

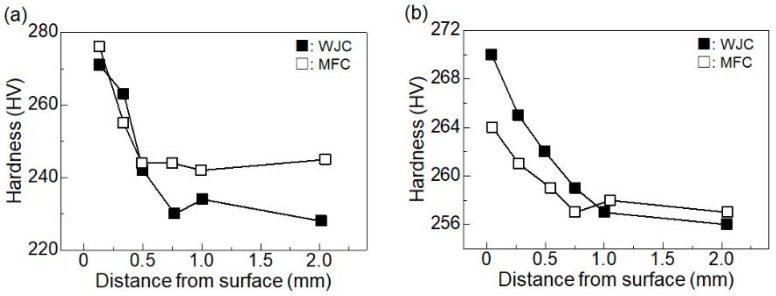

Figure 4. Hardness depth profile of the specimens after WJC and MFC treatment: (a) SCM435 and (b) SNCM630.

Figure 5 shows surface photographs of SCM435 (a, b) and SNCM630 (c, d) specimens after processing. The specimen surface was painted with oil-based ink prior to processing to identify the peening positions. The condition of the ink coating showed that the diameter of the peened portion of SCM435 was 40.8 mm after WJC processing and 42.2 mm after MFC processing. The peened diameter of SNCM630 was 41.3 mm after WJC processing and 42.7 mm after MFC processing. Therefore, MFC produced a slightly larger area than WJC produced. In addition, when the processed specimens were kept at room temperature for several months, corrosion developed after WJC processing, whereas there was almost no corrosion after MFC processing. Perhaps corrosion of the SNCM630 steel was prevented due to the formation of a dense oxide film on the specimen by increased temperature on the surface. Figure 6 shows OM micrographs of the SCM435 specimens after (a) WJC and (b) MFC. The particle size in the depth direction from the surface after each process was not significantly affected. In the near-surface region, no significant corrosion was observed after WJC processing, although it occurred easily after MFC processing. Corrosion was not observed in the ferrite phase but in the pearlite phase. The rust formed to a significant extent from the surface to a depth of approximately 1 mm.

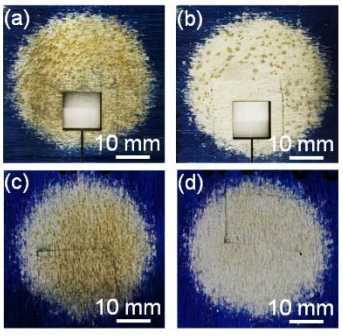

Figure 5. Surface change after treatment: of (a, c) WJC and (b, d) MFC. (a) and (b) are SCM435 and (c) and (d) are SNCM630.

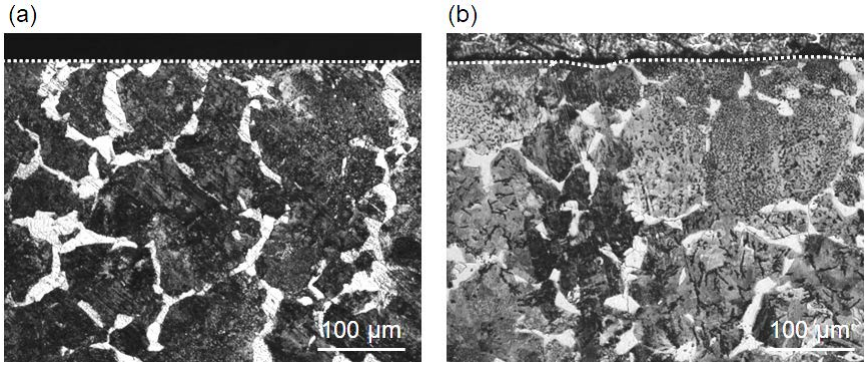

Figure 6. Optical micrographs of the SCM435 depth profile after (a) WJC and (b) MFC. A dotted line indicates a specimen surface.

Figure 7 shows SEM micrographs of the SNCM630 specimen depth profiles after WJC and MFC. The particle size in the depth direction from the surface after each process was not significantly affected. In the near-surface region, no significant corrosion was observed after WJC processing, although it occurred easily after MFC processing. Thus,

selective oxidation is considered to have occurred in the bulk of the MFC-processed specimen. The element that is easy to oxidize in this specimen is Cr, which migrates to the topmost surface and forms a Cr-poor region beneath the surface during heating by MFC processing. As a result, rust can be easily generated because the amount of Cr decreased in the near-surface region. The corrosion resistance of the specimen surfaces was assessed by measuring surface potentials, and the results are summarized in Table 3.

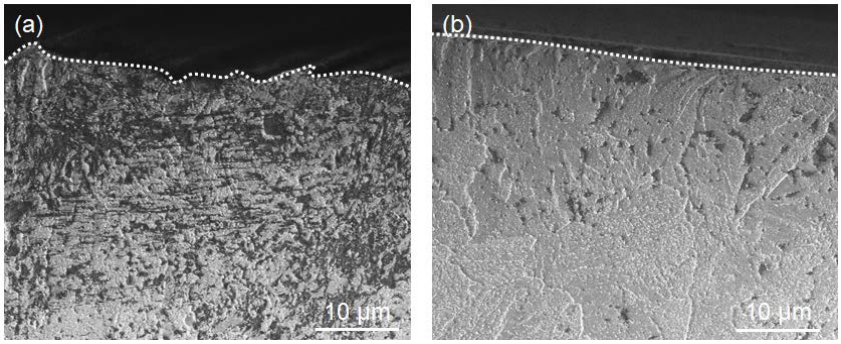

Figure 7. SEM images of the SNCM630 depth profile after (a) WJC and (b) MFC. A dotted line indicates a specimen surface.

Table 3. Surface potential of specimens after various treatments (mV).

	SCM435	SNCM630
As received	234 ± 14	359 ± 25
UC	194 ± 13	342 ± 18
WJC	382 ± 26	329 ± 18
MFC	544 ± 17	445 ± 16

The work function corresponding to the surface potential decreases as the surface roughness increases. The cavitation at the material surface during WJC generates impact pressures greater than several thousand megapascals. In addition, because some thermal energy is transferred to the material surface, a passive (corrosion-resistant) layer is formed. Soyama et al. [9] have also reported the formation of a passive layer as part of the mechanism by which the corrosion resistance of carbon steel is improved following the application of a cavitation jet. Regarding SNCM630, the surface potential of the WJC-processed specimen was lower than the abrasive material. It is probably influenced by the increase in surface defects compared with SCM435. During MFC, the bubbles generated by WJC (which are larger than UC bubbles) are irradiated with ultrasonic waves, and thus possess both high temperature (several thousand degrees Celsius) and high pressure (approximately 1,000 MPa). As these bubbles collide with the surface, a more stable passive layer is formed than that obtained with WJC. The reason for the selective oxidation inside the specimen during MFC processing was investigated by monitoring the water temperature, and Figure 8 summarizes the results. While UC did not increase the water temperature, both WJC and MFC did raise the temperature in the reactor. This occurred as a result of the pressurization of the water by the high-pressure pump, because the kinetic energy of the water was converted to thermal energy. From the viewpoint of bubble energy, it is thought that both WJC and MFC generate larger bubble collapse energies than UC processing, which also increases the water temperature. The slightly higher temperature obtained during MFC compared to WJC processing is due to the application of ultrasonic energy, reflecting the hot spots generated in the bubbles. Figure 9 plots the DO in the reactor over time for each processing method. The DO concentration was almost unchanged during UC, whereas it decreased during both WJC and MFC processing. In WJC processing, the pressure applied to the specimen surface increases due to the shock wave generated by the MJ. A part of the foam is deformed or bubbles become large again over a very short time span, and so both the water temperature and the temperature of the processed surface increase.

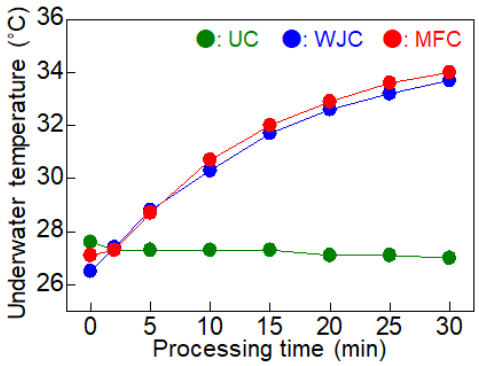

Figure 8. Relationship between processing time and underwater temperature.

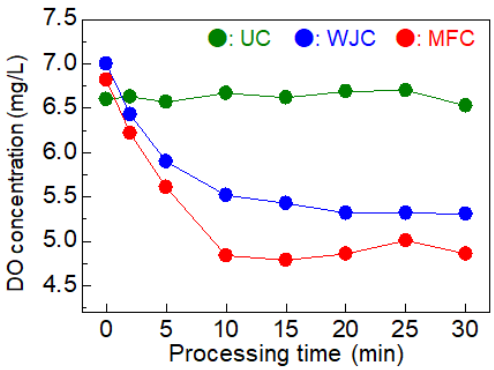

Figure 9. Relationship between processing time and DO concentration.

As a result, it is believed that DO combines with Cr to form oxides on the processed specimen surface, causing DO in the water to decrease. During MFC, the bubbles (which have a high internal temperature and pressure) increase the sample surface temperature to a greater extent than during WJC processing due to the hot-spot phenomenon inside the bubbles. Thus, the DO concentration is reduced to a greater degree as a passive layer is generated. As described above, in the MFC technique, bubbles having characteristically high temperature and high pressure collide with the specimen surface as the result of irradiating large bubbles generated by WJC with ultrasonic waves. This method effectively improves the surface residual stress via surface modification and also increases the specimen strength and corrosion resistance.

Conclusion

Improvements in residual stress and surface modification leading to high strength and corrosion resistance were found to occur at the surfaces of specimens processed with MFC. Corrosion resistance was improved via the formation of an oxide film by selective oxidation, as well as the reduction of surface defects. We concluded that this oxide film was formed by dissolved oxygen in the water reacting with Cr on the metal surface during the MFC treatment.

Acknowledgment

This work was supported by the Innovative Science and Technology Initiative for Security Program of the Acquisition, Technology & Logistics Agency (ATLA) of Japan.

References

[1] T. Yoshimura, K. Tanaka, N. Yoshinaga (2003). *Development of mechanical-electrochemical cavitation technology, Journal of Flow Engineering*. 20.
[2] D. Odhiambo, H. Soyama (2003). *Cavitation shotless peening for improvement of fatigue strength of carbonized steel*, J. Fatifue. 25.
[3] N. Saitou, K. Enomoto, K. Kurosawa, R. Morinaka, E. Hatashi, T. Ishikawa, T. Yoshimura (2003). *Development of water jet peening technique for reactor internal components nuclear power plant*. J. Jet Flow Eng 20.
[4] B. Gompf, R. Gunther, G. Nick, R. Pecha, W. Eisenmenger (1997). *Resolving sonoluminescence pulse width with time-correlated single photon counting*. Phys. Rev. Lett., 79.
[5] JP Lorimer, TJ Mason (1999). *Applications of Ultrasound in Electroplating in Electroplating, Electrochemistry*., 67.
[6] K. Tanaka, T. Yoshimura and N. Yoshinaga (2016). *Study on photocatalyst properties improvement of titanium oxide by the mechanical-electrochemical cavitation*. J. Jet Flow Eng 32.
[7] C. L. Kling and F. G. Hammitt (1972). *A photographic study of spark-induced cavitation bubble collapse*. J. Basic Eng 94.
[8] M. Ijiri, D. Shimonishi, D. Nakagawa, T. Yoshimura (2017). *Evolution of microstructure from the surface to the interior of Cr-Mo steel by water jet peening*. Materials Sciences and Applications 8.
[9] H. Soyama and M. Asahara (1999). *Improvement of the corrosion resistance of carbon steel surface by a cavitating jet*. J. Mater. Sci. Lett. 18 (5).